*Journal of Nano Research*
*ISSN: 1661-9897, Vol. 78, pp 31-42*

*Submitted: 2022-11-14*
*Revised: 2023-02-06*
*Accepted: 2023-02-06*
*Online: 2023-04-19*

# Synthesis and Characterization of $Ag/SiO_2$ Nanocomposite Based on Rice Husk Silica Using Sol-Gel Method

Junaidi[1,2,a*], Wiwin Sulistiani[1,b], Yessi Efridahniar[1,c], Indah Pratiwi[1,d], Iqbal Firdaus[1,e], Posman Manurung[1,f] and Pulung Karo Karo[1,g]

[1]Department of Physics, Faculty of Mathematics and Natural Sciences, Universitas Lampung, Bandar Lampung, Indonesia 35145

[2]Intrumentations Research Group, Department of Physics, Universitas Lampung, Bandar Lampung, Indonesia 35145

Email: [a*]junaidi.1982@fmipa.unila.ac.id (corresponding author); [b]wiwinsulistiani07@gmail.com; [c]yessiefridahniar019@gmail.com; [d]indah.pratiwi21@students.unila.ac.id; [e]iqbal.firdaus@fmipa.unila.ac.id; [f]posman.manurung@fmipa.unila.ac.id; [g]pulung.karokaro@fmipa.unila.ac.id

**Keywords:** silver, silica, rice husk, Uv-Vis, FTIR, XRD, SEM-EDX

**Abstract.** In this study, silver-silica ($Ag/SiO_2$) was synthesized using the sol-gel method by silica from rice husks. Silica derived from rice husk waste was previously synthesized using the sol-gel method. In addition, the Ag material used in this study was also performed into silver nanoparticles (AgNPs). This method was chosen to obtain an $Ag/SiO_2$ composite with nano size and high purity. AgNPs were synthesized using silver nitrate ($AgNO_3$) by reduction method at 90 $^oC$. The reducing agent and stabilizer used is trisodium citrate. UV-Vis, FTIR, XRD, and SEM-EDX were used to analyze $Ag/SiO_2$ composites. Uv-Vis analysis results $Ag/SiO_2$ has an absorption peak at a wavelength of 412 nm with a bandgap energy of 2.25 eV. These peaks indicate that AgNPs have formed in the $SiO_2$ membrane. The FTIR results revealed the Si-O-Si bonds which indicated the presence of silica and the Ag-O functional group, and the presence of AgNPs. The results of XRD analysis showed that the silica structure formed was cristobalite and silver crystals in the face center cubic (fcc) shape. The results of the SEM-EDX morphological analysis showed that the $Ag/SiO_2$ nanocomposite was shaped like sharp stone chips and the presence of small granules (granules) with different particle sizes and shapes, slightly porous and the composition of the compounds in the $Ag/SiO_2$ nanocomposite indicated the presence of various chemical elements in the sample, including carbon, oxygen, sodium, silica, and silver.

## Introduction

The role of nanostructures strongly influences almost all materials around. It‘s what makes nanoscale studies in physics exciting to work on. Nanomaterials describe a material whose structure is between 1 to 100 nm. One material that is of interest to many researchers and industry is silver (Ag). Silver has shown promising potential in various fields and has significantly contributed to the advancement of nanomaterials research. According to Tran et al., silver nanoparticles (AgNPs) have higher electrical and thermal conductivity than other metals [1]. The most widespread application of AgNPs is antibacterial [2] and antiviral in light of the COVID-19 pandemic [3]. AgNPs are also used in the textile industry in membrane filtration of water purifications [4], sensors [5], and catalysts [6].

There are several methods for synthesizing AgNPs, including the chemical reduction method. This method was chosen as the most effective method for producing AgNPs because it has advantages compared to other methods. The chemical reduction method is simpler, low cost, and can be used on a small scale [7]. Generally, the synthesis of AgNPs by the chemical reduction method requires metal precursors, reducing agents, and stabilizers. Stabilizing agents that are often used in the manufacture of silver nanoparticles include polyvinyl alcohol (PVA) and polyvinyl pyrrolidone (PVP) [8-9]. However, the AgNPs stabilized by the polymer added to the cost.

Therefore, synthesis without a stabilizing agent has attracted attention, as in previous studies using a reduction method using silver nitrate ($AgNO_3$) as a precursor and reducing agent trisodium citrate ($Na_3C_5H_6O_7$) which is also used as a stabilizer [10-12]. However, particle agglomeration is an obstacle for AgNPs [13-14]. Therefore, additional materials are needed to maximize the use of AgNPs.

One material that can be used to maximize the use of silver is silica ($SiO_2$). Silica is considered a material that has a high heat resistance and high chemical resistance [15]. Silica is proven to have properties that are proven to have high stability, chemical flexibility, and good biocompatibility [16]. In addition, silica is considered a cheap material because it can be found in abundance in the skin and leaves of plants, such as bagasse, corncobs and rice husks [17-19]. Based on research, rice husk has the highest silica content of around 99% [20].

In addition, silica material is a porous structure that can easily adsorb various ions and organic molecules in its pores and surfaces. Therefore, it is expected to be a suitable supporting material to maximize the use of AgNPs [21]. Many methods are used to make nanocomposites, including the sol-gel method [15]. The sol-gel method is known as a fairly easy and simple method because the synthesis is carried out at low temperatures and can produce high-purity and homogeneous materials.

Several studies on silver-silica ($Ag/SiO_2$) nanocomposites have been carried out, such as Kim et al. by producing AgNPs which form homogeneously on the surface of silica nanoparticles without experiencing aggression and showing excellent ability as an antibacterial agent [14]. Then in another study, the synthesis of silver silica nanocomposites based on tetraethyl orthosilicate (TEOS) was carried out using the sol-gel method by varying the sintering thermal treatment from 300 to 1 000 ºC which was then applied as an antibacterial agent [15]. The results of this study indicate that silver nanoparticles are distributed relatively homogeneously throughout the amorphous silica network with sizes from 20-40 nm after sintering at 800 ºC. $Ag/SiO_2$ nanocomposites have also been successfully carried out in this research [21]. The silver silica composite was subjected to thermal treatment up to 1 200 ºC. The results revealed that the $Ag/SiO_2$ nanocomposite structure was stable at 1 000 ºC. IR spectroscopy confirmed the predominant presence of the amorphous phase in the composite and silver embedded in the silica matrix. In addition, most of the silver content was found to decrease above 1 060 ºC, whereas above 1 110 ºC the silver in the sample was no longer detectable. This study concluded that to retain the silver AgNPs by Wysocka et al. reported that $Ag/SiO_2$ composites by mobilizing Ag into $SiO_2$ can reduce antibacterial concentrations [22].

This research is about the synthesis AgNPs into a $SiO_2$ matrix/membrane based on rice husk using the sol-gel method. The novelty of the research is the use of rice husk waste as a source of silica. Silica from rice husk in the form of sol has relatively high silica content and purity. Silica from rice husk also has enormous potential to be developed as a membrane because it has flexible and high mechanical strength. In addition, the Ag used is preformed into AgNPs through chemical reduction synthesis. This method is carried out so that the Ag used in the $Ag/SiO_2$ composite is ensured to be nano-sized [12]. The use of rice husk waste is one of the advantages in this study when compared to synthetic silica such as TEOS. TEOS has the disadvantage that it can damage the skin and cause blindness. This study also used aquadest solvent, which has economic value compared to ethanol etc.

## Materials and Methods

*Materials:* The materials used in the synthesis of $Ag/SiO_2$ are rice husk collected from local sources, silver nitrate ($AgNO_3$, Merck 99%), sodium hydroxide (NaOH, chemical product 90%), trisodium citrate ($Na_3C_6H_5O_7$, Merck 99%), nitric acid ($HNO_3$, chemical product 68%) deionized/distilled water was used.

*Methods:* Synthesis of $Ag/SiO_2$ was carried out in 4 steps. Firstly, the preparation of silica sol extraction from rice husks. Second, the synthesis of AgNPs using chemical reduction with the reaction equation as in Equation (1). Third, the synthesis of $Ag/SiO_2$ composites using the sol-gel method. Finally, the $Ag/SiO_2$ composite samples were characterized to see optical properties, crystal structure, morphology, and elemental content. The preparationof rice husk silica sol extraction is shown in Figure 1.

$$4Ag^{+} + C_6H_5O_7Na_3 + 2H_2O \rightarrow 4Ag^{0} + C_6H_5O_7H_3 + 3Na^{+} + H^{+} + O_2\uparrow \quad (1)$$

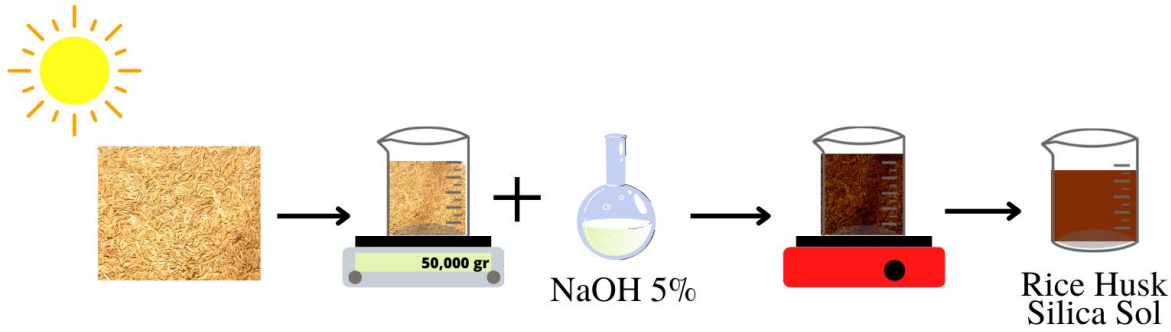


Figure 1. Preparation of rice husk silica sol extraction

The first step to obtaining a silica sol based on rice husks was washing the rice husks with clean water for 1 h. The floating rice husks were discarded, and the sinking ones were taken for use in further preparation. Rice husks were soaked again in hot water for 6 h. This is so that water-soluble impurities such as rice stalks, soil, dust, and other contaminants can be separated from the rice husks. After that, the rice husks were drained and dried in the sun. The dried rice husks were weighed as much as 50 g and dissolved in a solution of 500 ml of 5% NaOH. Rice husks submerged in NaOH solution are heated for ±30 minutes while stirring until boiling (100 ºC) and dark brown in color. The silica sol that was obtained was cooled by covering it with plastic wrap. Then the silica sol was allowed to stand for 24 h. Silica sol that had been set aside was filtered to obtain precipitate or rice husk extract. Figure 2 shows the synthesis of AgNPs using the reduction method.

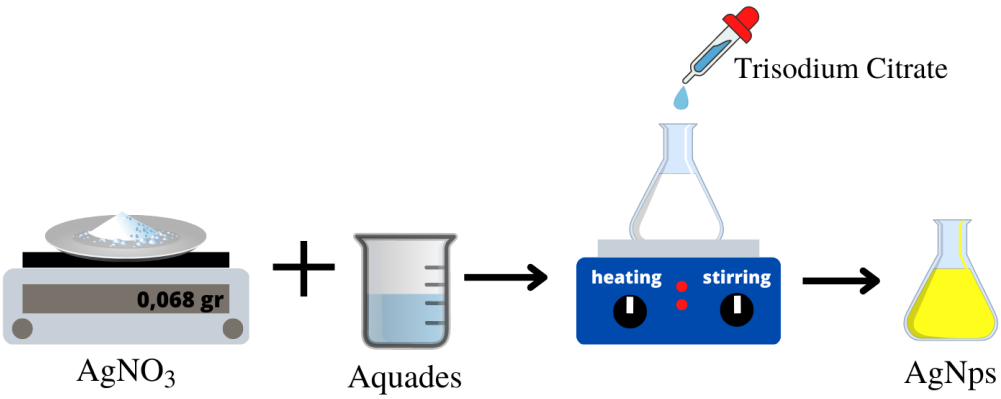


Figure 2. Synthesis of silver nanoparticles by reduction method.

Silver nanoparticles were prepared using $AgNO_3$ as a silver precursor and trisodium citrate as a reducing agent and stabilizer at 8 mM and 64 mM in distilled water, respectively. The $AgNO_3$ solution was heated at 90 ºC while stirring at 500 rpm. Trisodium citrate solution was injected into $AgNO_3$ solution for 2 minutes. Then started again for 15 minutes to obtain a resolution of AgNPs. The manufacturing of $Ag/SiO_2$ nanomaterials can be seen in Figure 3.

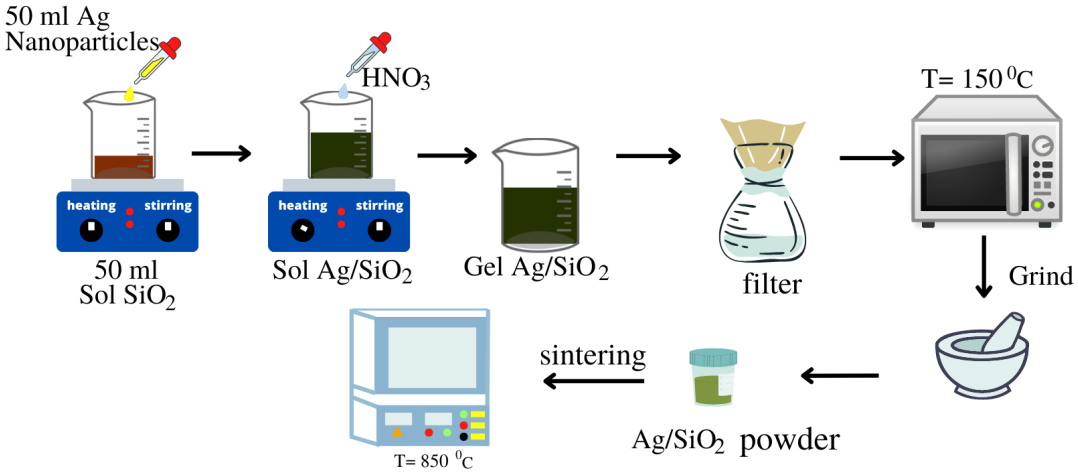


Figure 3. Synthesis of $Ag/SiO_2$ by using the sol-gel method.

The synthesis of $Ag/SiO_2$ was made in a ratio of 1:1 by mixing amount of 50 ml of distilled silica sol and 50 ml of AgNPs sol. Furthermore, $HNO_3$ with a concentration of 10% was injected into the $Ag/SiO_2$ sol to form a gel. Gel began aging for 24 h. The gel was washed with distilled water and filtered, and dried at 150 ºC. Furthermore, the solids formed are ground and sifted. Finally, $Ag/SiO_2$ powder was sintered at 850 ºC for characterization.

*Characterization:* The optical properties were assessed using UV-vis spectroscopy (Shimadzu, UV1700) at a wavelength of 300 to 800 nm. Functional group characteristics were used to identify a mixture of chemically bonded compounds and organic components of a material that could be analyzed using an FTIR spectrometer (Bruker ALPHA II) with an infrared spectrum in the middle region of the wave number range of 500 to 4 000 $cm^{-1}$. The phase structure of the silver silica composite sample was characterized using XRD (X'Pert Powder PW 30/40) with CuKα target (λ=1.542) with an angle of 3-90º. Morphological testing of $Ag/SiO_2$ samples was carried out using scanning electron microscopy (SEM, JEOL JSM-6510LA). The samples testing was carried out at 2 000×, 5 000×, and 10 000× magnifications. The chemical composition analysis was carried out using Energy Dispersive X-Ray (EDX) by an accuracy level of up to 0.1%.

## Results and Discussion

The relationship between absorbance value and wavelength was obtained to determine the absorption peak on the $Ag/SiO_2$ nanocomposites. The results of the UV-Vis $Ag/SiO_2$ analysis are shown in Figure 4.

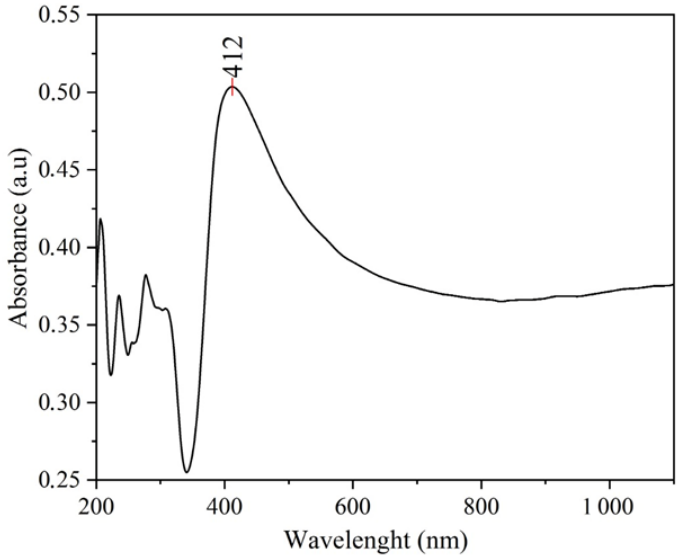


Figure 4. UV-Vis Spectra of $Ag/SiO_2$ nanocomposites.

Figure 4 shows the spectrum of the UV-Vis analysis of $Ag/SiO_2$ nanocomposites by a maximum absorption peak at a wavelength of 412 nm. These results are by studies that have been carried out with peak of $Ag/SiO_2$ from 380 to 450 nm. The resulting stable AgNPs are characterized by the formation of yellow colloidal silver [23].

In addition to the absorbance peak, UV-Vis was also used to determine the bandgap energy of $Ag/SiO_2$. The band gap energy was calculated through the reflectance spectra of the UV-Vis. The reflectance percentage was processed using the Kubelka-Munk theorem and the Tauc plot. The band gap energy measurements are shown in Figure 5.

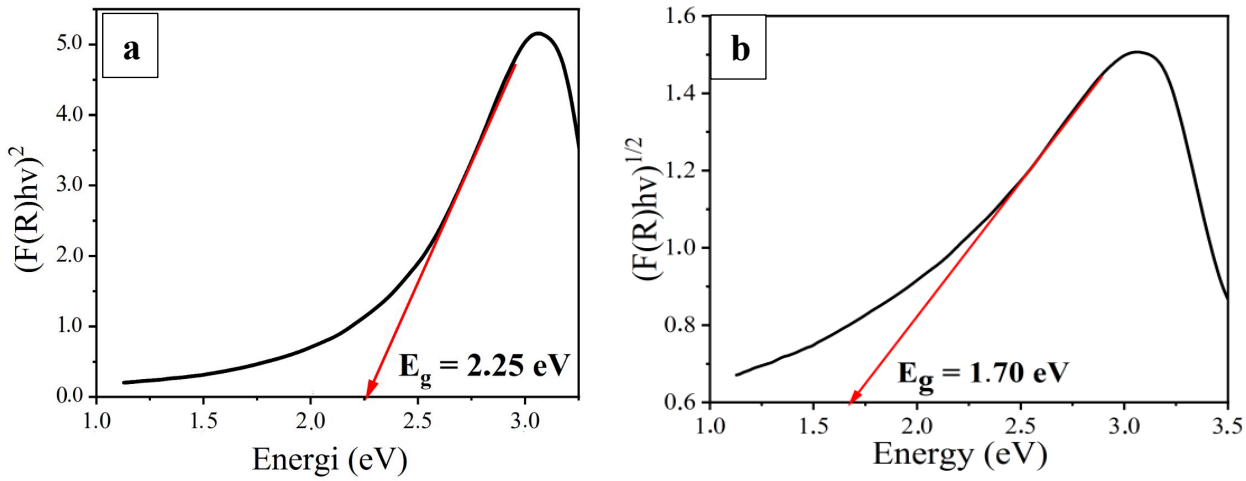


Figure 5. Bandgap energy of $Ag/SiO_2$ by (a) direct method and (b) indirect method.

Figure 5(a) shows that the direct bandgap of $Ag/SiO_2$ nanocomposites is 2.25 eV, and Figure 5(b) shows that the indirect band gap of $Ag/SiO_2$ nanomaterials is 1.70 eV. The band gap energy on silica is 8.06 eV [24]. The band gap energy for silver is 2.51 eV [25]. From the reference, the band gap energy of silver is around 3.16-3.41 eV (direct method) and about 2.81-3.01 eV (indirect method) [26]. For bandgap energy, the highest $Ag/SiO_2$ is 2.43-2.81 eV [27]. This band gap is equal to that obtained in a study by Li et al., which is 2.28-2.55 eV [28-31].

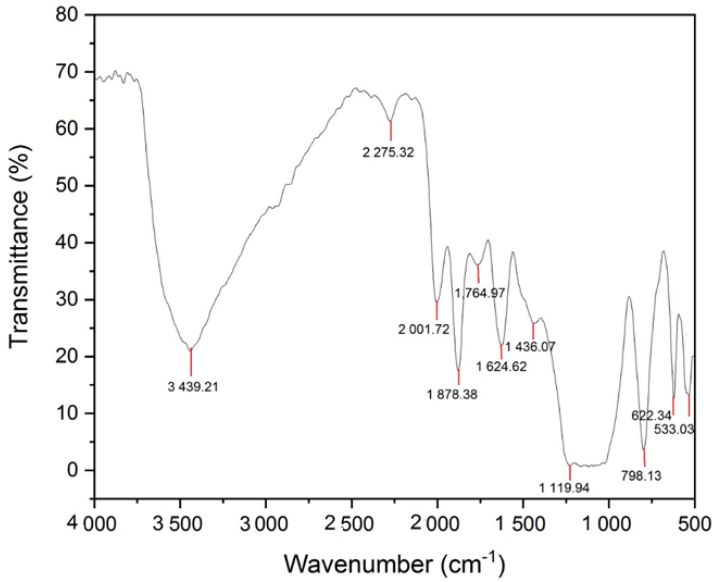


Figure 6. FTIR Spectrum of $Ag/SiO_2$.

In Figure 6, the peak at 3 439.21 $cm^{-1}$ is a typical peak for the stretching vibration of the –OH group (hydroxyl group). Thus, the silica used as the sample is believed to contain a hydroxyl group, indicating a Si–OH or silanol bond [32]. A peak reinforces this at 1 624.62 $cm^{-1}$, a bending vibration of the O-H group (hydrogen bond) and water molecules [33]. The peak of 2 275.32 $cm^{-1}$ is the

asymmetric strain of the isocyanate [34]. According to the peak, it shows the carbonyl group in the silica [32]. At the peak of 2 001.72 $cm^{-1}$ is the C-H functional group of alkanes [31]. Furthermore, the peak of 1 878.38 and 1 764.97 $cm^{-1}$ is the stretching vibration of C=O [22, 35]. Another peak of 1 436.07 $cm^{-1}$ is considered a sign of the presence of silver [12,15, 35]. The peak indicates the presence of silica functional group is at a peak of 1 119.94 $cm^{-1}$, which means the presence of a Si-O-Si siloxane active group [29, 32, 36] and at this peak corresponds to the asymmetric strain vibration of the bond Si-O-Si [37]. The presence of the Si-O-Si functional group is strengthened by the presence of a peak at 798.13 $cm^{-1}$, which is a symmetrical strain of Si-O-Si [31, 37] and. Furthermore, the peak at 622.34 $cm^{-1}$ shows the stretching of Si-O-Si [33]. Then the peak at 533.03 $cm^{-1}$ is considered a sign of the presence of the $Ag_2O$ spectrum [38,39] also states that at 600 $cm^{-1}$, wave number is the strain of oxygen metal (M-O). This result is similar to what has been shown by this also confirmed by Karthik et al., which states that at wave numbers from 600-400 $cm^{-1}$ is the Ag-O strain [32].

The $Ag/SiO_2$ nanocomposite structure was analyzed using the standard diffractogram source from Crystallography Open Database (COD). The XRD qualitative analysis was to determine the crystal structure. Furthermore, the data was analyzed by matching the sample data of the diffraction pattern graph with the database on the sample. The database obtained data in the form of crystal structures and lattice parameters. The results of the XRD diffractogram can be seen in Figure 7.

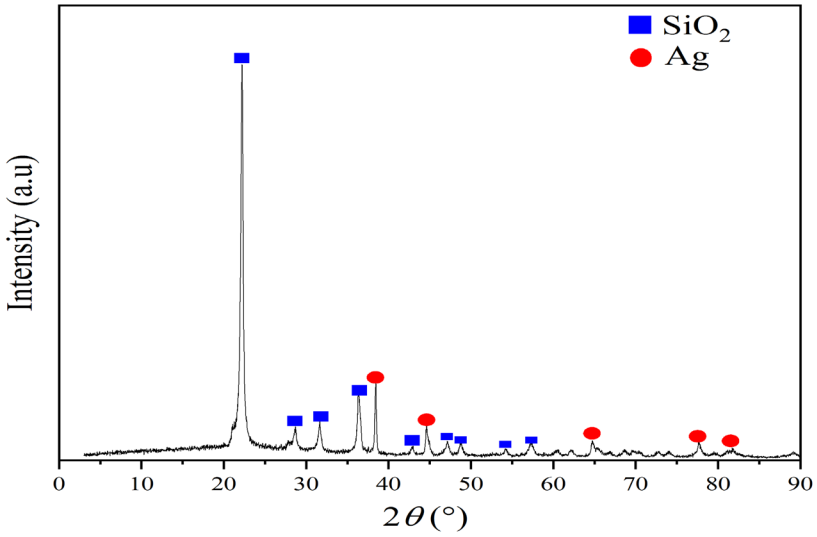


Figure 7. XRD diffractogram of $Ag/SiO_2$.

From Figure 7, it is known that the diffraction pattern of silica at peak 2θ = 22.19°, 28.68°; 31.62°; 36.3°; 42.87°; 47.18°; 48.71°; 54.17°; 57.30° indicates that the structure formed is cristobalite in the lattice plane (101), (111), (102), (200), (211), (113), (212), (203), (301). At the peak of 2θ = 21.45°, another phase was formed, namely tridymite (COD 96-901-3494). The tridymite and cristobalite phases of rice husk silica begin to form on heating above 800 C with 2θ = 22° and 36° [40].

The crystalline structure of silver is formed at 2θ = 38.43°; 44.60°; 65.06°; 77.69°; 81.86° in the lattice plane (111), (200), (202), (311), and (222) with the face center cubic (FCC) phase by previous studies [41]. According to research, this silver crystal peak appears most intensively found in the temperature range from 1 080 to 1 120 °C [22].

Through XRD diffractogram, data obtained can be used to determine the crystal size through the value of full width at half maximum (FWHM). The crystal size is calculated using the Scherer Equation as in Equation (2).

$$L = \frac{0.94\lambda}{B\cos\theta} \tag{2}$$

where $L$ is the crystal size (nm), $\lambda$ is the X-ray wavelength (Å), $\beta$ is the maximum half-peak width (rad), and $\theta$ is the peak center angle (°). The obtained crystal sizes of $Ag/SiO_2$ nanomaterials are shown in Table 1.

Table 1. The crystal size of $Ag/SiO_2$

| Element | $k$ (nm) | $\lambda$ (nm) | $\theta$ (°) | cos $\theta$ | $B$ (rad) | $L$ (nm) |
|---|---|---|---|---|---|---|
| $SiO_2$ | 0.94 | 0.15405 | 11.095 | 0.98 | 0.00535 | 27.50 |
| Ag | 0.94 | 0.15405 | 19.225 | 0.94 | 0.00329 | 46.50 |

To improve the search-match results obtained, further refinement is carried out based on the intensity of the X-ray diffraction pattern between the observational data using a structural model. The refinement results can be seen in Figure 8 and Table 2.

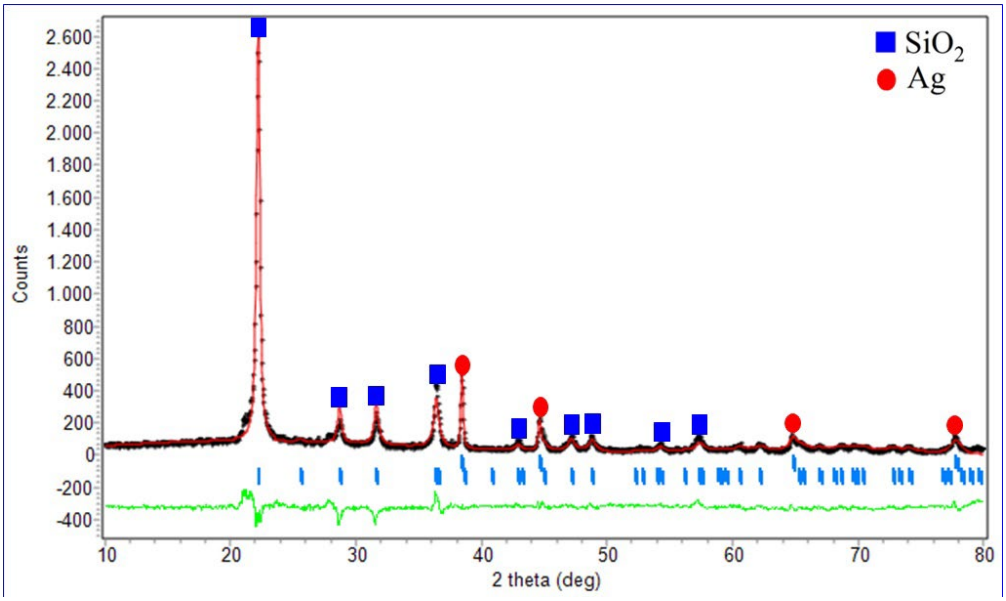


Figure 8. Refinement result of $Ag/SiO_2$.

Table 2. Percentage of conformity of XRD data refienement of $Ag/SiO_2$.

| Sample | $R_{wp}$(%) | $R_p$(%) | $R_{exp}$(%) | $GoF$(%) |
|---|---|---|---|---|
| $Ag/SiO_2$ | 9.03 | 12.94 | 13.43 | 0.59 |

Table 2 shows the output results of the refinement of $Ag/SiO_2$ samples with $R_{wp}$, $R_p$, $R_{exp}$ values of less than 20% and GoF values of less than 4%, indicating a value that is quite good for refinement and has conformity to the pattern with a model standard as Rietveld method [42]. As previously described, the GoF value of the $Ag/SiO_2$ nanomaterial sample is less than 4%. This means that the $SiO_2$ and Ag crystals have a relatively high structural similarity with the database of matching results obtained from the qualitative analysis. The refinement results for each phase parameter are shown in Table 3.

Table 3. Cell parameters of $Ag/SiO_2$

| Phase | $a$ (Å) | $b$(Å) | $c$(Å) | α(°) | β(°) | γ(°) |
|---|---|---|---|---|---|---|
| Ag | 4.0580 | 4.0580 | 4.0580 | 90 | 90 | 90 |
| $SiO_2$ | 4.9709 | 4.9709 | 6.9278 | 90 | 90 | 90 |

The matched cristobalite crystal with COD number 96-900-9687 has a tetragonal structure with a space group P 41 21 2 (92). Meanwhile, Ag crystals compared with COD number 96-901-1609, have a cubic system with a space group of F m 3 m (225). The unit cell volume of Ag is 66.82 $Å^3$, and the volume of silica cristobalite unit cells is 171.18 $Å^3$. The results are smaller than the study [40], which obtained a unit cell volume of Ag of 67.89 $Å^3$ and a unit cell volume of $SiO_2$ of 173.44 $Å^3$. It is

assumed that by decreasing the unit cell volume, the size of the crystallite formed may also be smaller, and the atomic density will be more significant [43]. Figure 9 shows the surface morphology of the $Ag/SiO_2$ from the SEM.

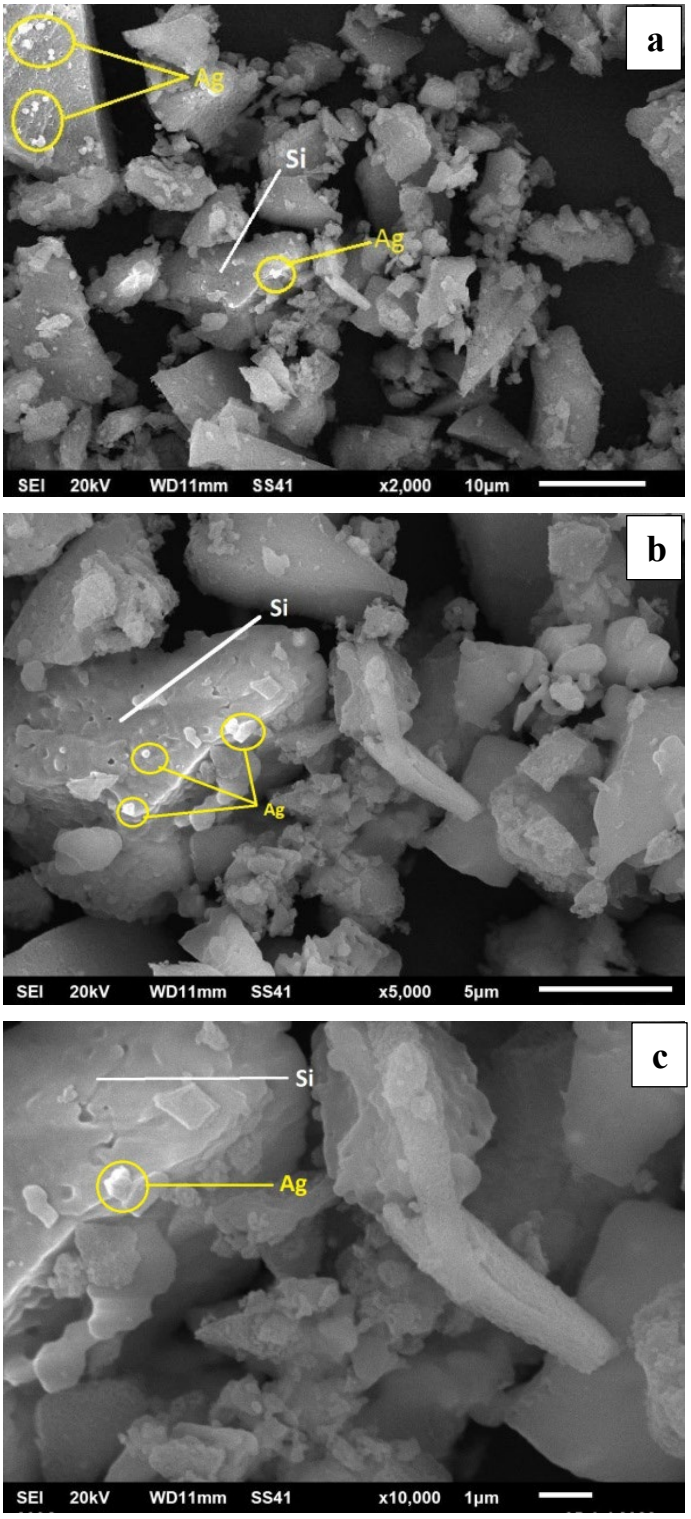


Figure 9. SEM image of $Ag/SiO_2$ at magnification (a) 2 000×, (b) 5 000×, and (c) 10 000×.

Figure 9 shows a solid with a shape like sharp stone flakes; it can be seen that there are small granules (granules) with different particle sizes and shapes, slightly porous. In addition, the microstructure shows differences in dark and light colors, which indicates that the sample consists of several elements for EDX analysis using an X-ray detector which aims to determine the factors present in the sample, as shown in Figure 10 and Table 4.

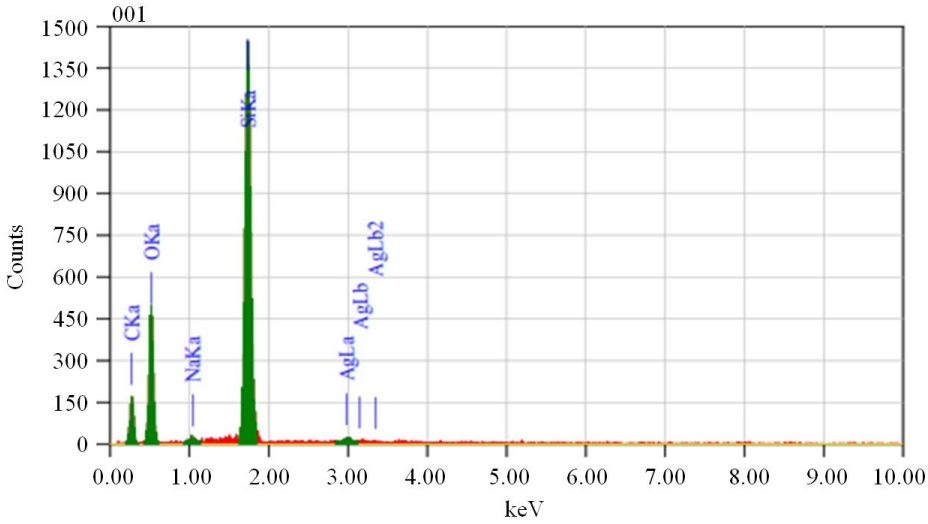


Figure 10. SEM-EDX of $Ag/SiO_2$

Table 4. Elemental of $Ag/SiO_2$ from SEM-EDX.

| Element | Content (%) | Atom (%) |
|---|---|---|
| C | 29.77 | 40.33 |
| O | 44.23 | 44.98 |
| Na | 0.41 | 0.29 |
| Si | 24.58 | 14.24 |
| Ag | 1.01 | 0.15 |

Additional information obtained from the analysis with SEM is EDX data, which shows the elements present in the sample and the sample's composition based on these elements. The results are presented in Table 4, which shows the presence of various chemical elements in the model, including C, O, Na, Si, and Ag.

## Conclusions

The synthesis of $Ag/SiO_2$ nanocomposite using the sol-gel method sintered at 850 $^oC$ has been successfully carried out. XRD results show that the silica structure formed is cristobalite at an angle of $2\theta = 22.19^o$, and silver crystals are face center cubic (fcc). The Uv-Vis of $Ag/SiO_2$ analysis results has an absorption peak at a wavelength of 412 nm, indicating AgNPs have been formed. The direct bandgap value is 2.25 eV, and the indirect bandgap is 1.70 eV. The FTIR results show that there are Si-O-Si bonds which indicate the presence of silica, and the Ag-O functional group, which indicates the presence of silver. The results of the SEM-EDX morphological analysis showed that the $Ag/SiO_2$ nanocomposite was shaped like sharp stone chips and the presence of small granules (granules) with different particle sizes and shapes, slightly porous and the composition of the compounds in the $Ag/SiO_2$ nanocomposite indicated the presence of various chemical elements. The sample includes carbon, oxygen, sodium, silica, and silver. This research has the potential to be developed as a membrane for anti-bacterial applications.

## Acknowledgment

This work was supported by a research grant of Basic Research, Contract No. 666/UN26.21/PN/2022, by the Ministry of Research, Technology and Higher Education of the Republic of Indonesia via the Institute for Research and Community Services of Universitas Lampung.

**References**

[1] Tran, Q. H., Nguyen, V. Q., and Le, A. T. Silver Nanoparticles: Synthesis, Properties, Toxicology, Applications and Perspectives. Nanoscience and Nanotechnology. 4 (2013) 1–20.

[2] Zaman, Y., Ishaque, M. Z., Sattar, R., Rehman, M. M., Saba, I., Kanwal, S., Akram, M., Shahzad, M., Kanwal, H., Qadir, R., and Siddique, A. B. Antibacterial Potential of Silver Nanoparticles Synthesized Using Tri-Sodium Citrate Via Controlled Exploitation of Temperature. Digest Journal of Nanomaterials and Biostructures. 17 (2022) 979–987.

[3] Jeremiah, S. S., Miyakawa, K., Morita, T., Yamaoka, Y., and Ryo, A. Potent Antiviral Effect of Silver Nanoparticles on SARS CoV-2. Biochemical and Biophysical Research Communications. 533 (2020) 195–200.

[4] Salem, S., and Fouda, A. Green Synthesis of Metallic Nanoparticles and Their Prospective Biotechnological Applications. Biological Trace Element Research.199 (2021) 344–370.

[5] Imran, M., Ehrhardt, C. J., Bertino, M. F., Shah, M. R., and Yadavalli, V. K. Chitosan Stabilized Silver Nanoparticles for The Electrochemical Detection of Lipopolysaccharide: A Facile Biosensing Approach for Gram-Negative Bacteria. Micromachines. 11 (2020) 413–417.

[6] Paul, D., Sachan, D., and Das, G. Silver Nanoparticles Embedded On In-Vitro Biomineralized Vaterite: A Highly Efficient Catalyst With Enhanced Catalytic Activity Towards 4-Nitrophenol Reduction. Molecular Catalysis. 504 (2021) 1–9.

[7] Quintero-Quiroz, C., Acevedo, N., Zapata-Giraldo, J., Botero, L.E., Quintero, J., Zárate-Triviño, D., Saldarriaga, J., and Pérez, V.Z. Optimization of Silver Nanoparticle Synthesis by Chemical Reduction and Evaluation of Its Antimicrobial and Toxic Activity. Biomaterials Research. 23 (2019) 1-15.

[8] Iravani, S., Korbekandi, H., Mirmohammadi, S.V., and Zolfaghari, B. Synthesis of Silver Nanoparticles: Chemical, Physical and Biological Method. Research in Pharmaceutical Sciences. 9 (2014) 385–406.

[9] Gudikandula, K., and Maringanti, S.C. Synthesis of Silver Nanoparticles by Chemical And Biological Methods and Their Antimicrobial Properties. Journal of Experimental Nanoscience. 11 (2016) 714-721.

[10] Aashritha, S. Synthesis of Silver Nanoparticles by Chemical Reduction Method and Their Antifungal Activity. International Research Journal of Pharmacy. 4 (2013) 111-113.

[11] Sertbakan, T.R., Al-Shakarchi, E.K., and Mala, S.S. The Preparation of Nano Silver by Chemical Reduction Method. Journal of Modern Physics. 13 (2022) 81-88.

[12] Junaidi. Spektrofotometer UV-Vis Untuk Estimasi Ukuran Nanopartikel Perak. Jurnal Teori dan Aplikasi Fisika. 5 (2017) 97–102.

[13] Badiah, H. I., Seedeh, F., Supriyanto, G., & Zaidan, A. H. Synthesis of Silver Nanoparticles and the Development in Analysis Method. IOP Conference Series: Earth and Environmental Science. 217 (2019) 1–8.

[14] Kim, Y. H., Kim, C. W., Cha, H. G., Jo, B. K., Ahn, G. W., Hong, E. S., & Kang, Y. S. Preparation of Antibacterial Silver-Containing Silica Nanocomposite. Surface Review and Letters. 15 (2008)117–122.

[15] Pham, D. P., Huynh, K. K., Tran, C. V., Vu, V. Q., and Tran, T. T. Van. Preparation and Structural Characterization of Sol-Gel-Derived Silver Silica Nanocomposite Powders. International Journal of Materials Science and Applications. 3 (2014) 147–151.

[16] Sembiring, S., and Karo-Karo, P. Pengaruh Suhu Sintering Terhadap Karakteristik Termal dan Mikrostruktur Silika Sekam Padi. Jurnal Sains MIPA. 13 (2007) 233–239.

[17] Affandi, S., Setyawan, H., Winardi, S., Purwanto, A., & Balgis, R. A Facile Method For Production of High-Purity Silica Xerogels from Bagasse Ash. Advanced Powder Technology. 20 (2009) 468–472.

[18] Dai, S., Lei, H., and Fu, J. Self-assembly preparation of Popcorn-Like Colloidal Silica and Its Application on Chemical Mechanical Polishing of Zirconia Ceramic. Ceramics International. 46 (2020) 1-6.

[19] Simanjuntak, W., Sembiring, S., Pandiangan, K. D., Syani, F., & Situmeang, R. T. M. The Use of Liquid Smoke as A Substitute for Nitric Acid for Extraction of Amorphous Silica From Rice Husk Through Sol-Gel Route. Oriental Journal of Chemistry. 32 (2016) 2079–2085.

[20] Yuvakkumar, R., Elango, V., Rajendran, V., & Kannan, N. High-Purity Nano Silica Powder From Rice Husk Using A Simple Chemical Method. Journal of Experimental Nanoscience. 9 (2014) 272–281.

[21] Jia, H., Hou, W., Wei, L., Xu, B., & Liu, X. The Structures and Antibacterial Properties of no-$SiO_2$ Supported Silver/Zinc-Silver Materials. Dental Materials. 24 (2008) 244–249.

[22] Dudek, K., Podwórny, J., Dulski, M., Nowak, A., and Peszke, J. X-ray Investigations Into Silica/Silver Nanocomposite. Powder Diffraction. 32 (2017) 82–86.

[23] Mohd, N. K., Khalik, W. M. A. W. M., and Azmi, A. A. Synthesis and Characterization of Silica-Silver Core-Shell Nanoparticles. Malaysian Journal of Analytical Sciences. 23 (2019) 290–299.

[24] Prabha, S., Durgalakshmi Lichtfouse, D., Rajendra, S., and Lichtfouse, E. Plant-Derived Silica Nanoparticles and Composites for Biosensors, Bioimaging, Drug Delivery and Supercapacitors: Environmental Chemistry Letters. 19 (2021) 1667–1691.

[25] Shukla, S. K. Rice Husk Derived Adsorbents for Water Purification. Environmental Chemistry for a Sustainable World. 38 (2020) 131–144.

[26] Aziz, A., Khalid, M., Akhtar, M. S., Nadeem, M., Gilani, Z. A., Khan, M.N., Rehman, J., Ullah, Z., and Saleem, M. Structural, Morphological and Optical Investigations of Silver Nanoparticles Synthesized By Sol-Gel Auto-Combustion Method. Digest Journal of Nanomaterials and Biostructures. 13 (2018) 679–683.

[27] Sahar, M. R., and Yusoff, N. M. The Influence of Silver Nanoparticles on Optical Properties of Samarium Doped Magnesium Tellurite Glasses. In Materials Today: Proceedings. (2015) 5117-5121.

[28] Rahman, U. A., Geng, J., Rehman, S., Jin, R., Liang, X., and Zhu, W. On Semi-Classical Optical Reponse of Metallic Silver and Silver Coated Silica Nanoparticles. Sixth Asia-Pacific Conference on Antennas and Propagation. 1 (2018) 1–3.

[29] El-Sheshtawy, H. S., Ghubish, Z., Shoueir, K. R., and El-Kemary, M. Activated $H_2O_2$ on $Ag/SiO_2–SrWO_4$ Surface for Enhanced Dark and Visible-Light Removal Of Methylene Blue and p-nitrophenol. Journal of Alloys and Compounds. 842 (2020) 1-12.

[30] Assis, M., Simoes, L. G. P., Tremiliosi, G. C., Coelho, D., Minozzi, D. T., Santos, R. I., Vilela, D. C. B., do Santos, J. R., Ribeiro, L. K., Rosa, I. L. V., Mascaro, L. H., Andres, J., and Longo, E. $SiO_2$-Ag Composite as a Highly Virucidal Material: A Roadmap That Rapidly Eliminates SARS-CoV-2. Nano Material. 11 (2021) 1–19.

[31] Li, H., Wang, M., Li, Y., Mo, F., Zhu, L., Li, Z., Xu, J., Kong, Y., Deng, N., and Chai, R. Adsorption Characteristics of Silver Atoms and Silver Ions on Silica Surface in Silver Nanoparticle Hydrosol System. Applied Surface Science. 562 (2021) 1-8.

[32] Sembiring, S., Riyanto, A., Firdaus, I., Junaidi, and Situmeang, R. Structure and Properties of Silver-Silica Composite Prepared from Rice Husk Silica and Silver Nitrate. Ceramics-Silikáty. 66 (2022) 185–195.

[33] Karthik, C., Caroline, D. G., Dhanam, M.P., and Prabha, S.P. Synthesis, Characterization of Ag-$SiO_2$ Nanocomposite and Its Application in Food Packaging. Journal of Inorganic and Organometallic Polymers and Materials. 31 (2021) 2532–2541.

[34] Adam, F., Ahmed, A. E., and Min, S. L. Silver Modified Porous Silica From Rice Husk and Its Catalytic Potential. Journal of Porous Materials. 15 (2008) 433–444.

[35] Bayu, A., Nandiyanto, D., Oktiani, R., and Ragadhita, R. How to Read and Interpret FTIR Spectroscope of Organic Material. Indonesian Journal of Science & Technology. 1 (2019) 97–118.

[36] Jeon, H. J., Yi, S. C., and Oh, S. G. Preparation and Antibacterial Effects of Ag-$SiO_2$ Thin Films by Sol-Gel Method. Biomaterials. 24 (2003) 4921–4928.

[37] Daifullah, A.M., Girgis, B., and Gad, H.M. Utilization of Agro Residues (Rice Husk) in Small Waste Water treatment Plants. Materials Letter. 57 (2003) 1723-1731.

[38] Wysocka, K., Olsztynska, S., Plesch, G., Plecenik, A., Podbielska, H., and Bauer, J. Nano-Silver Modified Silica Particles in Antibacterial Photodynamic Therapy. Applied Surface Science. 461 (2018) 260-268.

[39] Simanjuntak, W., Sembiring, S., Pandiangan, K. D., Syani, F., and Situmeang, R. T. M. The Use of Liquid Smoke As A Substitute For Nitric Acid For Extraction of Amorphous Silica From Rice Husk Through Sol-Gel Route. Oriental Journal of Chemistry. 32 (2016) 2079–2085.

[40] Duhan, S., Devi, S., and Srivastava, M. Characterization of Nanocrystalline Ag/$SiO_2$ Nanocomposites And Synthesis By Wet Chemical Method. Indian Journal of Pure and Applied Physics, 48 (2010) 271–275.

[41] Shinohara, Y., and Kohyama, N. Quantitative Analysis of Tridymite and Cristobalite Crystallized in Rice Husk Ash by Heating. Industrial Health. 42 (2004) 277–285.

[42] Kisi, E. Rietveld Analysis of Powder Difraction Patterns. Material Forum. 18 (1994) 135–153.

[43] Navas-Bachillera, M., Persoons, T., and D'Arcy, D. M. Exploring Bulk Volume, Particle Size and Particle Motion Definitions to Increase The Predictive Ability of In Vitro Dissolution Simulations. European Journal of Pharmaceutical Sciences. 71 (2022) 106185.